HHS Public Access

Author manuscript

J Neurochem. Author manuscript; available in PMC 2021 January 01.

Published in final edited form as:

J Neurochem. 2020 November ; 155(3): 300–312. doi:10.1111/jnc.15032.

Cathepsin B inhibition blocks neurite outgrowth in cultured neurons by regulating lysosomal trafficking and remodeling

Muzhou Jiang[1], **Jie Meng**[3], **Fan Zeng**[1], **Hong Qing**[4], **Gregory Hook**[5], **Vivian Hook**[6], **Zhou Wu**[1,2,*], **Junjun Ni**[1,4,*]

[1]Department of Aging Science and Pharmacology, Faculty of Dental Science, Kyushu University, Fukuoka 812-8582, Japan

[2]OBT Research Center, Faculty of Dental Science, Kyushu University, Fukuoka 812-8582, Japan

[3]Department of Neurology, West China Hospital, Sichuan University, Chengdu 610041, China

[4]Key Laboratory of Molecular Medicine and Biotherapy in the Ministry of Industry and Information Technology, Department of Biology, School of Life Science, Beijing Institute of Technology, Haidian District, Beijing 100081, China

[5]American Life Science Pharmaceuticals, La Jolla, CA, USA

[6]Skaggs School of Pharmacy and Pharmaceutical Sciences, University of California, San Diego, La Jolla, CA, USA

Abstract

Lysosomes are known to mediate neurite outgrowth in neurons. However, the principal lysosomal molecule controlling that outgrowth is unclear. We studied primary mouse neurons *in vitro* and found that they naturally develop neurite outgrowths over time and as they did so the lysosomal cysteine protease cathepsin B (CTSB) mRNA levels dramatically increased. Surprisingly, we found that treating those neurons with CA-074Me, which inhibits CTSB, prevented neurites. As that compound also inhibits another protease, we evaluated a N2a neuronal cell line in which the CTSB gene was deleted (CTSB KO) using CRISPR technology and induced their neurite outgrowth by treatment with retinoic acid. We found that CTSB KO N2a cells failed to produce neurite outgrowths but the wild-type (WT) did. CA-074Me is a cell permeable prodrug of CA-074, which is cell impermeable and a specific CTSB inhibitor. Neurite outgrowth was and was not suppressed in WT N2a cells treated with CA-074Me and CA-074, respectively. Lysosome-associated membrane glycoprotein2 (LAMP2)-positive lysosomes traffic to the plasma cell

[*]**Correspondence:** Zhou Wu, PhD. Department of Aging Science and Pharmacology, OBT Research Center, Faculty of Dental Science, Kyushu University, Fukuoka 812-8582, Japan. TEL: +81 92 642 6414; zhouw@dent.kyushu-u.ac.jp, Junjun Ni, PhD. Key Laboratory of Molecular Medicine and Biotherapy in the Ministry of Industry and Information Technology, Department of Biology, School of Life Science, Beijing Institute of Technology, Haidian District, Beijing 100081, China. TEL: +86 17600397519; nijunjun@bit.edu.cn.

Open Science Badges

This article has received a badge for *Open Materials* because it provided all relevant information to reproduce the study in the manuscript. More information about the Open Science badges can be found at https://cos.io/our-services/open-science-badges/

membrane in WT but not in CTSB KO N_2a cells. Interestingly, no obvious differences between WT and CTSB KO N2a cells were found in neurite outgrowth regulatory proteins, PI3K/AKT, ERK/MAPK, cJUN and CREB. These findings show that intracellular CTSB controls neurite outgrowth and that it does so through regulation of lysosomal trafficking and remodeling in neurons. This adds valuable information regarding the physiological function of CTSB in neural development.

Keywords

Neuron; Neurite outgrowth; Cathepsin B; Lysosomes

Introduction

Neurons begin their life as simple spheres and then ultimately assume an elaborate morphology with numerous, highly arborized dendrites and long axons. Neurites are defined as any projection from the soma of a neuron that can be either an axon or a dendrite. *In vitro*, neurons follow a developmental program that is reproducible under equivalent cell culture conditions. During neuron development, neurons have a spherical shape and typically begin extending lamellipodia and filopodia protrusions, where the neurites emerge and extending away from the cell soma (Flynn 2013). The initiation and elongation of neurites depend on the precisely regulated polymerization, convergence and crosslinking of actin filaments, which can be regulated by multiple signaling pathways including phosphoinositide 3-kinase/ protein kinase B (PI3K/AKT) (Lopez-Carballo *et al.* 2002), extracellular signal-regulated kinase/ mitogen activated protein kinase (ERK/MAPK) (Masia *et al.* 2007), cJUN (Dragunow *et al.* 2000) and cAMP response element-binding protein (CREB) (Chen *et al.* 2018). Interestingly, lysosomal exocytosises have been proven to regulate the long-term structural plasticity of dendritic spines by triggering matrix metalloproteinase 9 (MMP-9) activation and axonal outgrowth through exocytosis of the cysteine protease cathepsin B (EC3.4.22.1, CTSB) extracellular matrix remodeling (Padamsey et al. 2017; Tran et al 2018).

Lysosomes are degradative organelles that contain cathepsin (CTS) proteases. In addition to the classical functions of CTS for protein degradation through proteolysis of peptide bonds, there has been renewed interest in the modulator actions of CTS which generate activate substrates by specific cleavages (Nakanishi 2003; Terada *et al.* 2010; Sun *et al.* 2012; Wu *et al.* 2013). The lysosomal cysteine protease CTSB has been shown to play multiple roles in normal and pathological processes in brain. Normal functions of lysosomes participate in activity-dependent dendritic spine growth by calcium-mediated CTSB exocytosis which activates MMP-9 involved in extracellular matrix remodeling (Padamsey *et al.* 2017). Secretion of lysosomal CTSB enhances axonal outgrowth in neurons through degradation of chondroitin sulfate, the major axon inhibitory matrix (Tran *et al.* 2018). Furthermore, neuronal activity positions lysosomes at dendritic spines to facilitate synaptic plasticity through protein degradation at the junctions of dendrites and axons (Goo *et al.* 2017).

During brain pathological processes of injury, neurodegeneration, neuroinflammation, and related, loss of lysosomal integrity through membrane permeability leakage is associated with detrimental cognitive impairment and neuropathology. It has been reported that CTSB chronically activates nuclear factor-κB (NFκB) through the degradation of inhibitor of κBα (IκBα) in hypoxic-ischemic microglia (Ni *et al.* 2015). In addition, CTSB plays a critical role in Alzheimer's disease-like pathologies induced by chronic systemic exposure to lipopolysaccharide derived from *Porphyramonas gingivalis* (the major periodontal bacteria) in middle-aged mice, including chronic neuroinflammation, amyloid β accumulation in neurons and cognitive impairment (Wu *et al.* 2017). In a mouse model of Alzheimer's disease (APP/Lon), knockout of the CTSB gene results in improved memory deficits and amelioration of brain neuropathology (Kindy *et al.* 2012). Furthermore, lysosomal leakage of CTSB is involved in degrading mitochondrial transcription factor A in aged microglia (Ni *et al.* 2019).

These observations demonstrate the critical physiological roles of CTSB in neuronal development of dendrites and axons of synapses, which are known to become dysfunctional in brain injury and neurodegenerative diseases (Masliah 1995; Taoufik *et al.* 2018). To advance understanding of the role of CTSB in regulating synaptic dendritic and axonal features modeled by neuritic outgrowth in cultured neurons, this study investigated the regulation of CTSB in neurite formation by genetic deletion or pharmacological inhibition of CTSB in primary cultures of mouse brain cortical neurons and mouse N2a neuroblastoma cells. Results showed that lysosomal CTSB was responsible for the neurite growth through the regulation of lysosome trafficking and remodeling at the base of neurite growth cones.

Materials and methods

All reagents in the present study were purchased within 2 years and stored properly according to the manufactures. All experiments were performed and repeated according to the same time schedule. The same person performed the experiments and analysis, hence not being blinded to experimental conditions.

Cell culture

The mouse neuroblastoma cell line N2a (CCL-131, ATCC; RRID: CVCL_0470) was maintained in DMEM (Nissui, Cat#532–05915) containing 10% fetal bovine serum (Gibco, Cat#16010142) supplemented with 10 μg/ml insulin (Sigma, Cat#I5500), 1% penicillin-streptomycin (Gibco, Cat#15140122), 200 mM L-glutamine (Gibco, Cat#25030149) and 1 mg/ml glucose (Sigma, Cat#07-0680-5) at 37°C in a humidified atmosphere with 5% CO_2. The maximum number of passages for cell lines was 20. The study was not pre-registered. The cell line N2a (CCL-131, ATCC; RRID: CVCL_0470) was not listed as a commonly misidentified cell line by the International Cell Line Authentication Committee, and it was purchased in 2017 from ATCC. We didn't perform any authentications after purchase.

Primary neurons were prepared from the mouse neonatal cortex in accordance with the previously described methods (Ni *et al.* 2015). All experimental procedures of this study were approved by the Animal Care and Use Committee of Kyushu University (A27-232-0). In brief, there were 3 independent dissections in total, resulting in 9 wells per treatment.

Neonatal C57BL/6 mice of 2 days age after birth were purchased from Japan SLC, Inc. Mice of either sex were used in the present study. Neocortices from 30 pups were pooled together. The pups were euthanized by decapitation after cold-induced anesthesia, and their brains rapidly removed. Cryoanesthesia abolished perception of pain of pups. Neocortical tissues were dissected in ice cold Hank's buffer and subjected to enzymatic digestion using the Neural Tissue Dissociation Kit (Miltenyi Biotec, Cat#130-092-628). The single-cell suspensions were obtained after application to a 30-mm cell strainer. Cells were counted and seeded on glass coverslips pre-coated with 500 μg/mL poly-L-lysine (Sigma-Aldrich, Cat#P1399) and were cultured with MEM (Gibco, Cat#11090–081) containing 10% horse serum (ThermoFisher, Cat#16050122) supplemented with 1 mg/mL glucose (Sigma, Cat#07-0680-5), 1% penicillin-streptomycin (Gibco, Cat#15140122) and 100 mM sodium pyruvate (Gibco, Cat#11360-070) over night. On the next day after seeding, the medium was replaced with Neurobasal (Gibco, Cat#21103-049) supplemented with 2% B27 (Gibco, Cat#17504-044), 1mg/mL glucose (Sigma, Cat#07-0680-5), 1% penicillin-streptomycin (Gibco, Cat#15140122) and 200mM L-glutamine (Gibco, Cat#25030-081). There are thirty neonatal were used in the primary culture experiments without any exclusion. The experimental timelines are shown in Fig.1.

Generation of CTSB knock out cells

A neuronal CTSB knockout (CTSB KO) cell line was established by using N2a cells and a commercially available clustered regularly interspaced short palindromic repeats (CRISPR) and homology-directed repair (HDR) (ORIGENE, Cat#KN303984) on N2a cells via CRISPR and HDR. Positive cells were selected with 2 μg/ml puromycin (InvivoGen, Cat#ant-pr) for 15 days. A single cell clone was picked up and continued to culture. CTSB expression was assessed by Q-PCR and immunoblotting. During the generation, we also included scramble control gRNA (SKU GE100003, ORIGENE, Cat#KN303984) to serve as a negative control. Positive clones were collected and cultured. However, some positive cell gene KO may occur in one allele (heterozygous). To exclude heterozygous cells, 10 positive single clones were subjected to RT-PCR and Western blotting for further selection. The homozygous cells were confirmed and used in the subsequent experiments.

Immunoblotting analyses

The Wild-type (WT) and CTSB KO N2a cells were cultured at a density of 2×10^5 cells/ml in 6-well plates and differentiated by treatment with 20 μM all-trans retinoic acid (RA, Sigma, Cat#R2625). Cells were collected at indicated time points after differentiation. The immunoblotting analyses were conducted as described previously (Ni *et al.* 2019). In brief, cell lysates were electrophoresed using 12% sodium lauryl sulfate-polyacrylamide gels and protein on the SDS gels was electrophoretically transferred to polyvinylidene difluoride membranes. Following blocking with 5% nonfat milk, the membranes were incubated at 4°C overnight under gentle agitation with each primary antibody: mouse anti-CTSB (1:1000; Santa Cruz Biotechnology, RRID: AB_10842446), mouse anti-CTSS (1:1000; Santa Cruz Biotechnology, RRID:AB_10676822), mouse anti-CTSL (1:1000; Santa Cruz Biotechnology, Cat#sc-393770), mouse anti-CTSD (1:1000; Santa Cruz Biotechnology, RRID:AB_2827539), rabbit anti-p-ERK (1:1000; Cell Signaling, RRID:AB_331772); rabbit anti-ERK (1: 1000; Cell Signaling, RRID:AB_330744); rabbit anti-p-AKT (1:1000; Cell

Signaling, RRID:AB_329826); rabbit anti-AKT (1:1000; Cell Signaling, RRID:AB_331414); rabbit anti-p-cJUN (1:1000; Abcam, RRID:AB_726899); rabbit anti-p-CREB (1:1000; Cell Signaling, RRID:AB_2561044) and mouse anti-actin (1:5000; Abcam, RRID:AB_722536). After washing, the membranes were incubated with corresponding secondary antibodies labeled with horseradish peroxidase for 2 h at room temperature, washed and developed with a chemiluminescence detection system (Immubilon ECL Ultra Western HRP Substrate; Millipore, Cat#WBULS0100) with an image analyzer (LAS-1000; Fuji Photo Film).

Immunofluorescent staining

The Wild-type (WT) and CTSB KO N2a cells were seeded on coated glasses at a density of 10^5 cells/ml in 24-well plates and differentiated by treatment with 20 μM all-trans RA. 10 μM CA-074Me (L-3-trans-(Propylcarbamoyl)oxirane-2-carbonyl]-L-isoleucyl-L-proline Methyl Ester, CAS Number 147859-80-1, from PEPTIDE, Cat#4323-v) and 10 μM CA-074 (L-3-trans-(Propylcarbamyl)oxirane-2-carbonyl)-L-isoleucyl-L-proline, CAS Number 134448-10-5, from PEPTIDE, Cat#4322-v) were applied 2 h before RA. Cells were fixed with 4% paraformaldehyde at indicated time points. They were then incubated with the mouse anti-CTSB (1:1000; Santa Cruz Biotechnology, RRID: AB_10842446), rabbit anti-LAMP2 (1:1000; Abcam, RRID: AB_470550) and Neuron-Chrom™ Pan Neuronal Marker (1:1000; Millipore, RRID:AB_10953966) which reacts against key somatic, nuclear, dendritic, and axonal proteins distributed across the pan-neuronal architecture. After incubation with primary antibodies at 4°C overnight, the cells were washed and incubated with donkey anti-goat 488 (1:1000; Jackson ImmunoResearch, RRID:AB_2747389), donkey anti-mouse Cy3 (1:1000; Jackson ImmunoResearch, RRID:AB_2340813), and donkey anti-rabbit Cy3 (1:1000; Jackson ImmunoResearch, RRID:AB_2307443), then incubated with Hoechst (1:200, Sigma-Aldrich, Cat#14533) and mounted in Vectashield anti-fading medium (Vector Laboratories, Cat#H-1000). The fluorescent images were observed using a confocal laser scanning microscopy (CLSM, C2si, Nikon).

Inhibitors

10 μM pepstatin (PEPTIDE, Cat#4397) was used to inhibit CTSD, 10 μM Z-FL-COCHO (Calbiochem, Cat#219393) was used to inhibit CTSS, 10μM Z-FF-FMK (Cat#sc-364671) was used to inhibit CTSL and 10 μM CA-074Me (PEPTIDE, Cat#4323-v) was used to inhibit CTSB. It was noted that CA-074Me was reported to be selective for CTSB at concentration below 1μM and concentrations (more than 10μM) will be needed to inhibit CTSB; However, high concentration of CA-074Me inhibited CTSs broadly (Orlowski *et al.* 2015).

F-actin staining

The N2a cells were seeded on coated glasses at a density of 10^5 cells/ml in 24-well plates and differentiated by treatment with 20 μM all-trans RA for 2h after pretreatment with 10 μM pepstatin, 10 μM Z-FL-COCHO, 10μM Z-FF-FMK and 10 μM CA-074Me. The same concentration of inhibitors were also applied to the primary neurons 12h after seeding into the 24 well plates. Cells were fixed with 4% paraformaldehyde for 30min. After washing with PBS, cells were incubated with Texa Red-X Phalloidin (1 unit/well; Thermo Fisher

Scientific, Cat#T7471) for 1h and then with Hoechst stain (1: 200) and mounted in Vectashield anti-fading medium (Vector Laboratories, Car#H1000). The fluorescent images were observed using a CLSM (C2si, Nikon). The images were captured by NIS-Elements Viewer at the dimension of 1024 ×1024 (3 comps 12bit). Three channel series were applied as DAPI (emission wavelength, 447; excitation wavelength, 408), FITC (emission wavelength, 525; excitation wavelength, 488) and TRITC (emission wavelength, 785; excitation wavelength, 561).

Quantification of neurite outgrowth

To count the number of cells with neurites and measure neurite length, cells were stained with Neuron-Chrom™ Pan Neuronal Marker (1:1000; Millipore, RRID: AB_10953966). We scored for the number of cells with neurites which were greater than two cell body diameters in length in 0.05 mm^2. Six random fields were examined from each well and each experiment was repeated three times. For the quantification of lamellipodia, filopodia and growth cone in N2a cells and primary neurons, the thin protrusion were defined as filopodia, the sheet-like membrane protrusions were defined as lamellipodia, and the tips of neurites were defined as growth cones.

Real-time quantitative PCR analysis

The mRNA isolated from cells were subjected to a real-time quantitative PCR. The total RNA was extracted with RNAiso Plus (Takara, Japan, Cat#9108) according to the manufacturer's instructions. 1μg RNA was reverse transcribed to cDNA using the QuantiTect Reverse Transcription Kit (Qiagen, Japan, Cat#205311). After an initial denaturation step at 95°C for 5 min, temperature cycling was initiated. Each cycle consisted of denaturation at 95°C for 5 s, annealing at 60°C for 10 s, and elongation for 30 s. In total, 40 cycles were performed. The cDNA was amplified in duplicate using a Rotor-Gene SYBR Green RT-PCR Kit (Qiagen, Japan, Cat#204174) with a Corbett Rotor-Gene RG-3000A Real-Time PCR System. The data were evaluated using the RG-3000A software program (version Rotor-Gene 6.1.93, Corbett). The sequences of primer pairs are described below. CTSB: 5'-GCAGCCAACTCTTGGAACCTT-3' and 5'-GGATTCCAGCCACAATTTC TG-3', CTSD: 5'-CTGAGTGGCTTCATGGGAAT-3' and 5'-CCTGACAGTGGAGAAGGAGC-3', CTSS: 5'-CATCTTTGGAGTGAGCACCA-3' and 5'-GCATCCAAAACAGCCATCTTA-3', CTSL: 5'-ATGGCACGAATGAGGAAGAG-3' and 5'-GAAAAAGCCTCCCCTTCTTG-3', Actin: 5'-AGAGGGAAATCGTGCGTGAC −3'and Actin: 5'-CAATAGTGATGACCTGGCCGT-3'. For normalization, an endogenous control (actin) was assessed to control for the cDNA input, and the relative units were calculated by a comparative Ct method. All of the real-time RT-PCR experiments were repeated three times, and the results were presented as the means of the ratios ± SEM.

Statistical analysis

The data are represented as the means ± SEM. All data presented represent the mean of at least three replicates of independent cell culture preparations. The statistical analyses were performed by one-way ANOVA tests and student's t tests using the GraphPad Prism 7 software package. A value of $p < 0.05$ was considered to indicate statistical significance (GraphPad Software). There were no animals or cell preparations excluded from the analysis

in the present study. Assessment of the normality of data distribution was by Shapiro-Wilk normality test using GraphPad Prism 7 software package; No test for outliers was conducted on the data; no data points were excluded.

Results

Lysosomal cathepsins were increased during the maturation of primary neurons

Lysosomes are involved in the development of neurite extensions during neuronal maturation (Arantes & Andrews 2006) which is dependent on lysosomal enzymes, including cathepsins. Thus, we first set the research question with the aim of examining the expression of cathepsins during the maturation of neurons. The mRNA levels of CTSs including CTSB, CTSD, CTSS and CTSSL, were examined at 6 time points after seeding of primary cortical neurons in culture over 12 days. The mRNA levels of CTSs were significantly increased during the maturation of neurons (Fig. 2A–D). It was noted that the expression of CTSB was approximately 300-fold higher at day 12 in comparison to that at day 1(Fig. 2A), while the expression levels of CTSD, CTSS and CTSL increased approximately 100-fold, 80-fold and 170-fold respectively (Fig. 2 B–D). These increases in CTSs expression, especially the very large increase in CTSB, suggested that CTSB, CTSD, CTSS and CTSL may be involved in the maturation of neurons, which promoted us to examine the protein expression level of these CTSs in primary neurons during maturation. As expected, the protein expression level of CTSs were significantly increased during the maturation of neurons ((Fig. 2 E–I). To clarify the roles of CTSB, CTSD, CTSS and CTSL in neurite elongation, primary neuron cultures were pretreated with inhibitors of these CTSs. After 12 days of culture, cells treated with pepstatin, Z-FL-COCHO and Z-FF-FMK grew appreciable neurites as determined by F-actin staining (Fig. 2J, K). Surprisingly, cells treated with CA-074Me showed reduced neurite formation (Fig. 2J, K). Taken together, these results suggested CTSB may be essential for neurite outgrowth.

Increased CTSB was located in somas and neurites in N2a cells

N2a neuroblastoma cells do not naturally differentiate but can be induced to do so by treatment with 20 μM retinoic acid (RA) (Wang *et al.* 2010). To assess the expression of CTSB in N2a cells after treatment with RA, the mRNA and protein levels of CTSB were examined. The mRNA level of CTSB was significantly increased at 12 h, which was the first time point, and for all remaining time points up to 48 hours after RA treatment (Fig. 3A). Furthermore, the density of the band corresponding to mature CTSB protein increased significantly from 24 h to 48 h after RA treatment (Fig. 3B, C). Next, the localization of CTSB was examined by double immunofluorescent staining. In N2a cells without RA treatment, punctate CTSB signals were observed in somas and were well co-localized with LAMP2 (Fig. 3D). After treatment with RA for 48 h, enhanced punctate CTSB signals were detected in both somas (cell bodies) and neurites of N2a cells (Fig. 3E). These results suggested that increased CTSB is associated with both the initiation and elongation of neurite outgrowth in N2a cells.

Knockout of CTSB in N2a cells resulted in deficiency of neurite growth during differentiation

CA-074Me inactivates both CTSB and CTSL within living cells (Montaser *et al.* 2002). To exclude the possibility that CA-074Me inhibited neurite outgrowth through CTSL inhibition, we used CRISPR and HDR targeting CTSB to knockout (KO) CTSB in N2a cells. Real-time quantitative PCR demonstrated that CRISPR could efficiently reduce the expression of CTSB in N2a cells (Fig. 4A). Furthermore, Western blotting showed that the band corresponding to CTSB disappeared in CTSB KO cells (Fig. 4B). The CTSB KO cells were then used in the subsequent experiments. RA treatment resulted in visible changes in neurite outgrowth (appearance of processes longer than two cell bodies). The number of cells bearing neurites were examined. As reported previously (Wang *et al.* 2010), N2a cells constantly increased the number and length of neurites at 24 to 48 h after treatment with RA (Fig. 4C, D). In contrast, the neurite outgrowth was completely inhibited in CTSB KO N2a cells after treatment with RA (Fig. 4C, D). This result suggests that CTSB is involved in neurite outgrowth.

CTSB was critical in the initiation of neurite outgrowth

As a neurite primarily emerges out of the soma and then extends, CTSB was proven to be located in both somas and neurites. Thus, we first checked the effect of CTSB on the neurite outgrowth initiation stage. The N2a cell line was used and differentiated by treatment with RA. At 2 h after differentiation, N2a cells formed a spherical shape and lamellipodia and filopodia protrusions began extending (Fig. 5A). Pretreatment with pepstatin, Z-FL-COCHO and Z-FF-FMK had no effect on the formation of lamellipodia, filopodia or growth cone in N2a cells at 2 h after differentiation; however, CA-074Me significantly inhibited the lamellipodia, filopodia and growth cone formation (Fig. 5B). Moreover, primary cortical neurons were also used to examine the effects of these inhibitors on the neurite outgrowth. We found pepstatin, Z-FL-COCHO and Z-FF-FMK had no effect on the formation of lamellipodia, filopodia or growth cone in primary neurons at DIV1 (Fig. 5C, D); however, CA-074Me significantly inhibited the filopodia and growth cone formation (Fig. 5C, D). It was noted that Z-FF-FMK treated primary neurons showed less neurites compared to none-treatment group (Fig. 5C). Z-FF-FMK has been reported to inhibit cysteine protease, therefore Z-FF-FMK may partially inhibit CTSB in the present study. These results suggested that CTSB plays a critical role in neurite formation which is reflected in the inhibition of growth cone building in the initiation stage of the neurite.

Intracellular, but not secretory CTSB was responsible for neurite outgrowth

It has been reported that back propagating action potentials triggered the release of Ca^{2+} from lysosomes in hippocampal pyramidal dendrites (Padamsey *et al.* 2017). This Ca^{2+} release resulted in the exocytosis of the lysosomal CTSB, which activated MMP9 to maintain activity-dependent spine growth (Padamsey *et al.* 2017). Thus, the effect of CTSB on neurite outgrowth may have also resulted from secretory CTSB. To examine this possibility, we compared cell-permeable CA-074Me and cell non-permeable CA-074 both of which inhibit CTSB. The compounds were administered 2 h before RA treatment in N2a cell culture. RA treatment resulted in a visible increase in the number and length of neurites

number and length at 24 h until 48 h after treatment with RA (Fig. 6A, B). In contrast, neurite outgrowth was completely inhibited by CA-074Me in N2a cells after treatment with RA (Fig. 6A, B). The results confirmed the data obtained from CTSB KO N2a cells. Furthermore, CA-074 treatment had no effect on neurite outgrowth, shown by the same increase in the number and length of neurites as was observed in N2a cells that were treated with RA (Fig. 6A, B). These observations suggest that intracellular, but not secretory CTSB, is involved in the neurite outgrowth in N2a cells.

CTSB deficiency had no effect on signaling pathways regulating neurite outgrowth

It has been reported that neurite outgrowth was regulated by a series of signaling pathways including PI3K/Akt, ERK/MAPK, cJUN and CREB, which were activated by RA treatment (Chen *et al.* 2018; Dragunow *et al.* 2000; Lopez-Carballo *et al.* 2002; Masia *et al.* 2007). We investigated whether these signaling pathways were effected by CTSB deficiency. Phosphorylation of ERK, AKT, cJUN and CREB were examined in WT and CTSB KO N2a cells at 0, 5, 15, 30, 60, 120 and 240 min after RA treatment by Western blotting. Treatment of N2a cells with RA resulted in the rapid phosphorylation of ERK, AKT, cJUN and CREB. The phosphorylation of ERK, AKT and cJUN peaked at 30 min, while the phosphorylation of CREB peaked at 60 min (Fig. 7A–D). On the other hand, the phosphorylation of ERK, AKT, cJUN and CREB was also observed in CTSB KO N2a cells following RA treatment. The times of peak cJUN and CREB phosphorylation did not differ from that in WT N2a cells, while ERK and AKT phosphorylation peaked at 60 min after RA treatment (Fig. 7 E–H). Overall, these results indicated that the inhibition of neurite outgrowth by CTSB deficiency was not dependent on the change in the regulation signaling pathways.

CTSB deficiency blocked lysosomal trafficking to the leading edge of neuritic outgrowths

CTSB is a typical cysteine protease in lysosomes, and lysosomes are reported to regulate the structural plasticity of dendritic spines through exocytosis (Padamsey *et al.* 2017). Thus, we aimed to examine the effect of CTSB deficiency on lysosomal trafficking at the initiation stage of neurite outgrowth. At 2 h after treatment with RA, the punctate staining signals of CTSB and lysosome associated membrane protein-2 (LAMP2) were well co-localized and located at the neuritic edge of N2a cells (Fig. 8A). Furthermore, co-staining of F-Actin and LAMP2 showed that all lysosomes distributed at the cell edge were located at the base of filopodia and lamellipodia in WT N2a cells after RA treatment (Fig. 8B). However, there was no obvious distribution of lysosomes at the neuritic cell edge in CTSB KO N2a cells after treatment with RA (Fig. 8B). Primary neurons were used to further confirm the role of CTSB in lysosome distribution. We found that considerable lysosome were distributed to the neurites and also the base of growth cones (Fig.8C), however, knockdown CTSB by siRNA in primary neurons induced a cytosol distribution of lysosomes (Fig.8C). Moreover, knockdown of CTSB in primary neurons blocked the outgrowth of neurites, which further confirms the data obtained from N2a cells (Fig.8C). These results indicate that CTSB is critical in lysosome trafficking and remodeling during the initiation stage of neurite outgrowth.

Discussion

The major finding of the present study was that intracellular CTSB is involved in the initiation of neurite outgrowth via the regulation of lysosomal trafficking and remodeling in cultured neurons (summarized in Fig. 8D). To our knowledge, this is the first study to add valuable information regarding the physiological roles of CTSB in the earliest phase of neuronal differentiation and development.

The functions of CTSB have been studied by others using various methods including CTSB overexpression, knock down and KO mice for many years. Recently, CRISPR was used to target CTSB in mammalian cancer cells (Gnanamony & Gondi 2018, Caculitan *et al.* 2017) and in mouse macrophages (Wang *et al.* 2020), but we believe this is the first report of a neuronal CTSB KO cell line generated using CRISPR. This provided a useful tool for studies of CTSB function, because the CTSB KO cells showed the permanent non-expression of CTSB, and have the advantages of being rapidly available and stable.

Neurite growth is a critical event in the development of nervous system, which requires both extracellular and intracellular pathways, and endosomes/lysosomes have been reported to mediate neurite extensions by their exocytosis (Arantes & Andrews 2006). During brain development, CTSB is a ubiquitously expressed lysosomal cysteine protease (Hsu *et al.* 2018) which is involved in neurobiological functions. We detected the increased expression of CTSB in the somas and neurites of N2a cells during development, suggesting that CTSB may be involved in neurite formation and extension. Using CTSB KO N2a cells, we observed no neurites during neuron development. These data demonstrated that CTSB was controlling the processes of neurite outgrowth in these cells. The expression level of CTSB mRNA has a large difference between the primary cortical neurons and N2a cells in our present culture system. A study comparing N2a cells to primary neurons found that N2a cells were much less sensitive to neurotoxins, possibly due to a lack of important membrane receptors and ion channels (LePage *et al.* 2005). It is reasonable to consider that primary neurons may have a higher CTSB mRNA expression during differentiation compared to N2a cells. On the other hand, the protein expression level of CTSB during the maturation of N2a and primary neuron did not exhibit large differences (2.3 folds increase versus 2 folds increase).

It is of interest that CTSB KO mice are generally indistinguishable from their sufficient litter mates, are fertile (Reinheckel *et al.* 2001), and have the same neuromuscular performance as WT mice (Moon *et al.* 2016, Hook *et al.* 2014). It is known that numerous factors, mechanisms, and signaling pathways participate in neurodevelopment in vivo and, thus, such factors together with CTSB may participate in neuronal differentiation. Detailed investigation of synaptic dendrites and axons in CTSB KO mice will enhance understanding of CTSB in neural maturation. Nonetheless, CTSB KO mice exhibit subtle behavioral differences shown by lack of improvement in spatial memory with exercise (Moon, 2016), and female CTSB KO mice have slightly higher anxiety (Czibere *et al.* 2011). Notably, CTSL is essential for functions in CTSB KO mice because double CTSB and CTSL KO mice die shortly after birth and have several neurological abnormalities (Felbor *et al.* 2002).

Neurite outgrowth is regulated by intracellular signals, including PI3K/AKT (Lopez-Carballo *et al.* 2002), ERK/MAPK (Masia *et al.* 2007), cJUN (Dragunow *et al.* 2000) and CREB (Chen *et al.* 2018). To examine the effects of CTSB on the regulation signals, we observed the activation of signals including PI3K/Akt, ERK/MAPK, cJUN and CREB in WT and CTSB KO N2a cells treated with RA. No obvious difference was found in the activation of either cJUN or CREB between WT and CTSB KO N2a cells. This indicates that the involvement of CTSB deficiency in neurite outgrowth is independent of the PI3K/Akt, ERK/MAPK, cJUN and CREB signaling pathways.

Our findings showed that LAMP-2 positive lysosomes containing CTSB were trafficked to the base of the filopoidia and lamellipodia of the cultured WT N2a cells, but failed to be trafficked in CTSB KO N2a cells, which paralleled the defective neurites observed in CTSB KO N2a cells, indicating that CTSB is involved in the trafficking of LAMP-2 positive lysosomes from cytosol to the base of filopodia and lamellipodia, where the neurite outgrowth initiated. These results were supported by previous reports that showed that CTSB is involved in the trafficking of TNF-α containing vesicles to the plasma membrane in macrophages (Ha *et al.* 2008). In CTSB or CA-074Me-treated N2a cells, LAMP-2 positive lysosomes showed a defect in trafficking from cytosol to the base of filopodia and lamellipodia, supporting the hypothesis that CTSB is not involved in the cleavage functions at the plasma membrane. Furthermore, no effects on neurite growth were detected in the CatD inhibitor (Pepstatin), CTSL inhibitor (Z-FF-FMK) and CTSS inhibitor (Z-FL-COCHO)-treated N2a cells or primary cortical neurons, which indicates that the involvement of CTSB in controlling neurite outgrowth is specific. Remarkably, the inhibition effect of neurite outgrowth was only found in N2a cells treated with a cell-permeable CTSB inhibitor, but not in those treated with an inhibitor that was not cell-permeable. These results indicated an intracellular function of lysosomal CTSB in the neurite outgrowth of neurons. However, the present study could not delineate whether the action of CTSB occurred in the cytoplasm or other intracellular compartments, because unlike other CTSs, CTSB functions as an endopeptidase at neutral pH and is also found in extralysosomal sites, including the cytosol and plasma membrane (Schmitz *et al.* 2019). Therefore, further study is needed to clarify where CTSB functions during lysosome trafficking and neurite outgrowth.

The present findings provide evidence to support that CTSB is involved in the initiation of neurite outgrowth via the regulation of lysosomal trafficking and intracellular remodeling; however, it was recently reported that exocytosis of CTSB from lysosomes is involved in the regulation of the long-term structured plasticity of dendritic spines by extracellular matrix remodeling (Padamsey *et al.* 2017; Goo *et al.* 2017). The molecular mechanism through which CTSB intracellularly regulates lysosome trafficking and remodeling during the initiation of neurite outgrowth remains to be elucidated. In conclusion, our findings indicate that CTSB is involved in the initiation of neurite outgrowth through the regulation of lysosomal trafficking and remodeling in cultured neurons. Physiological benefits and pathological disadvantage need to be taken into account when considering CTSB intervention.

Acknowledgements and conflict of interest disclosure

This work is supported by the Japanese JSPS KAKENHI Grant Number 16K11478 (Grants-in-Aid for Scientific Research to Z.W.) and Beijing Institute of Technology Research Fund Program (Young Scholars to J.N.). Support has also been provided by the United States National Institute of Neurological Disorders and Stroke of the National Institutes of Health (NIH) under Award Numbers R41NS110147 (to G.H. and V.H.) and R01NS109075 (to V.H.), and the content is solely the responsibility of the authors and does not necessarily represent NIH official views.

Authors M. Jiang, J. Meng, F. Zeng, H. Qing, Z. Wu, and J. Ni declare that they have no conflict of interest. G. Hook is employed by and has equity in American Life Science Pharmaceuticals (ALSP). V. Hook has equity in ALSP; the terms of this arrangement has been approved by the University of California, San Diego in accordance with its conflict of interest policies.

Abbreviations

CREB	cAMP response element-binding protein
CTS	Cathepsin
CTSB	Cathepsin B
CTSD	Cathepsin D
CTSL	Cathepsin L
CTSS	Cathepsin S
CRISPR	Clustered regularly interspaced short palindromic repeats
CLSM	Confocal laser scanning microscopy
ECM	Extracellular matrix
HDR	Homology-directed repair
IκBα	Inhibitor of κBα
KO	Knockout
LAMP2	Lysosome associated membrane protein-2
MMP-9	Matrix metalloproteinase 9
NFκB	Nuclear factor-κB
PI3K/AKT	Phosphoinositide 3-kinase/protein kinase B
RA	Retinotic acid
RRID	Research Resource Identifiers
WT	Wild-type

References

Arantes RM and Andrews NW (2006) A role for synaptotagmin VII-regulated exocytosis of lysosomes in neurite outgrowth from primary sympathetic neurons. The Journal of neuroscience 26, 4630–4637. [PubMed: 16641243]

Caculitan NG, Dela Cruz Chuh J, Ma Y et al. (2017) Cathepsin B Is Dispensable for Cellular Processing of Cathepsin B-Cleavable Antibody-Drug Conjugates. Cancer research 77, 7027–7037. [PubMed: 29046337]

Chen L, Feng P, Peng A, Qiu X, Zhu X, He S and Zhou D (2018) cAMP response element-binding protein and Yes-associated protein form a feedback loop that promotes neurite outgrowth. Journal of cellular and molecular medicine 22, 374–381. [PubMed: 28857442]

Czibere L, Baur LA, Wittmann A et al. (2011) Profiling trait anxiety: transcriptome analysis reveals cathepsin B (Ctsb) as a novel candidate gene for emotionality in mice. PloS one 6, e23604. [PubMed: 21897848]

Dragunow M, Xu R, Walton M et al. (2000) c-Jun promotes neurite outgrowth and survival in PC12 cells. Brain research. Molecular brain research 83, 20–33. [PubMed: 11072092]

Felbor U, Kessler B, Mothes W, Goebel HH, Ploegh HL, Bronson RT and Olsen BR (2002) Neuronal loss and brain atrophy in mice lacking cathepsins B and L. Proceedings of the National Academy of Sciences of the United States of America 99, 7883–7888. [PubMed: 12048238]

Flynn KC (2013) The cytoskeleton and neurite initiation. Bioarchitecture 3, 86–109. [PubMed: 24002528]

Gnanamony M and Gondi CS (2018) Targeting the Expression of Cathepsin B Using CRISPR/Cas9 System in Mammalian Cancer Cells. Methods in molecular biology 1731, 123–131. [PubMed: 29318549]

Goo MS, Sancho L, Slepak N, Boassa D, Deerinck TJ, Ellisman MH, Bloodgood BL and Patrick GN (2017) Activity-dependent trafficking of lysosomes in dendrites and dendritic spines. The Journal of cell biology 216, 2499–2513. [PubMed: 28630145]

Ha SD, Martins A, Khazaie K, Han J, Chan BM and Kim SO (2008) Cathepsin B is involved in the trafficking of TNF-alpha-containing vesicles to the plasma membrane in macrophages. Journal of immunology 181, 690–697.

Hook GR, Yu J, Sipes N, Pierschbacher MD, Hook V and Kindy MS (2014) The cysteine protease cathepsin B is a key drug target and cysteine protease inhibitors are potential therapeutics for traumatic brain injury. Journal of neurotrauma 31, 515–529. [PubMed: 24083575]

Hsu A, Podvin S and Hook V (2018) Lysosomal Cathepsin Protease Gene Expression Profiles in the Human Brain During Normal Development. Journal of molecular neuroscience 65, 420–431. [PubMed: 30008074]

LePage T Dickey W Gerwick H Jester L and Murray F(2005) On the use of neuro-2a neuroblastoma cells versus intact neurons in primary culture for neurotoxicity studies. Critical Reviews in Neurobiology 17, 27–50. [PubMed: 16307526]

Lopez-Carballo G, Moreno L, Masia S, Perez P and Barettino D (2002) Activation of the phosphatidylinositol 3-kinase/Akt signaling pathway by retinoic acid is required for neural differentiation of SH-SY5Y human neuroblastoma cells. The Journal of biological chemistry 277, 25297–25304. [PubMed: 12000752]

Masliah E (1995) Mechanisms of synaptic dysfunction in Alzheimer's disease. Histology and histopathology 10, 509–519. [PubMed: 7599445]

Masia S, Alvarez S, de Lera AR and Barettino D (2007) Rapid, nongenomic actions of retinoic acid on phosphatidylinositol-3-kinase signaling pathway mediated by the retinoic acid receptor. Molecular endocrinology 21, 2391–2402. [PubMed: 17595318]

Montaser M, Lalmanach G and Mach L (2002) CA-074, but not its methyl ester CA-074Me, is a selective inhibitor of cathepsin B within living cells. Biological chemistry 383, 1305–1308. [PubMed: 12437121]

Moon HY, Becke A, Berron D et al. (2016) Running-Induced Systemic Cathepsin B Secretion Is Associated with Memory Function. Cell metabolism 24, 332–340. [PubMed: 27345423]

Nakanishi H (2003) Microglial functions and proteases. Molecular neurobiology 27, 163–176. [PubMed: 12777686]

Ni J, Wu Z, Peterts C, Yamamoto K, Qing H and Nakanishi H (2015) The Critical Role of Proteolytic Relay through Cathepsins B and E in the Phenotypic Change of Microglia/Macrophage. The Journal of neuroscience 35, 12488–12501. [PubMed: 26354916]

Ni J, Wu Z, Stoka V, Meng J, Hayashi Y, Peters C, Qing H, Turk V and Nakanishi H (2019) Increased expression and altered subcellular distribution of cathepsin B in microglia induce cognitive impairment through oxidative stress and inflammatory response in mice. Aging cell 18, e12856. [PubMed: 30575263]

Orlowski M, Colbert D, Sharma S, Bogyo M, Robertson A and Rock L (2015). Multiple Cathepsins Promote Pro-IL-1β Synthesis and NLRP3-Mediated IL-1β Activation. Journal of Immunology. 195, 1685–1697.

Padamsey Z, McGuinness L, Bardo SJ, Reinhart M, Tong R, Hedegaard A, Hart ML and Emptage NJ (2017) Activity-Dependent Exocytosis of Lysosomes Regulates the Structural Plasticity of Dendritic Spines. Neuron 93, 132–146. [PubMed: 27989455]

Reinheckel T, Deussing J, Roth W and Peters C (2001) Towards specific functions of lysosomal cysteine peptidases: phenotypes of mice deficient for cathepsin B or cathepsin L. Biological chemistry 382, 735–741. [PubMed: 11517926]

Schmitz J, Gilberg E, Loser R, Bajorath J, Bartz U and Gutschow M (2019) Cathepsin B: Active site mapping with peptidic substrates and inhibitors. Bioorganic & medicinal chemistry 27, 1–15. [PubMed: 30473362]

Sun L, Wu Z, Hayashi Y, Peters C, Tsuda M, Inoue K and Nakanishi H (2012) Microglial cathepsin B contributes to the initiation of peripheral inflammation-induced chronic pain. The Journal of neuroscience 32, 11330–11342. [PubMed: 22895716]

Taoufik E, Kouroupi G, Zygogianni O and Matsas R (2018) Synaptic dysfunction in neurodegenerative and neurodevelopmental diseases: an overview of induced pluripotent stem-cell-based disease models. Open biology 8.

Terada K, Yamada J, Hayashi Y, Wu Z, Uchiyama Y, Peters C and Nakanishi H (2010) Involvement of cathepsin B in the processing and secretion of interleukin-1beta in chromogranin A-stimulated microglia. Glia 58, 114–124. [PubMed: 19544382]

Tran AP, Sundar S, Yu M, Lang BT and Silver J (2018) Modulation of Receptor Protein Tyrosine Phosphatase Sigma Increases Chondroitin Sulfate Proteoglycan Degradation through Cathepsin B Secretion to Enhance Axon Outgrowth. The Journal of neuroscience 38, 5399–5414. [PubMed: 29760175]

Wang X, Meng D, Chang Q, Pan J, Zhang Z, Chen G, Ke Z, Luo J and Shi X (2010) Arsenic inhibits neurite outgrowth by inhibiting the LKB1-AMPK signaling pathway. Environmental health perspectives 118, 627–634. [PubMed: 20439172]

Wang F, Song Z, Chen J, Wu Q, Zhou X, Ni X and Dai J (2020) The immunosuppressive functions of two novel tick serpins, HlSerpin-a and HlSerpin-b, from Haemaphysalis longicornis. Immunology 159, 109–120. [PubMed: 31606893]

Wu Z, Ni J, Liu Y, Teeling JL, Takayama F, Collcutt A, Ibbett P and Nakanishi H (2017) Cathepsin B plays a critical role in inducing Alzheimer's disease-like phenotypes following chronic systemic exposure to lipopolysaccharide from Porphyromonas gingivalis in mice. Brain, behavior, and immunity 65, 350–361.

Wu Z, Sun L, Hashioka S, Yu S, Schwab C, Okada R, Hayashi Y, McGeer PL and Nakanishi H (2013) Differential pathways for interleukin-1beta production activated by chromogranin A and amyloid beta in microglia. Neurobiology of aging 34, 2715–2725. [PubMed: 23831373]

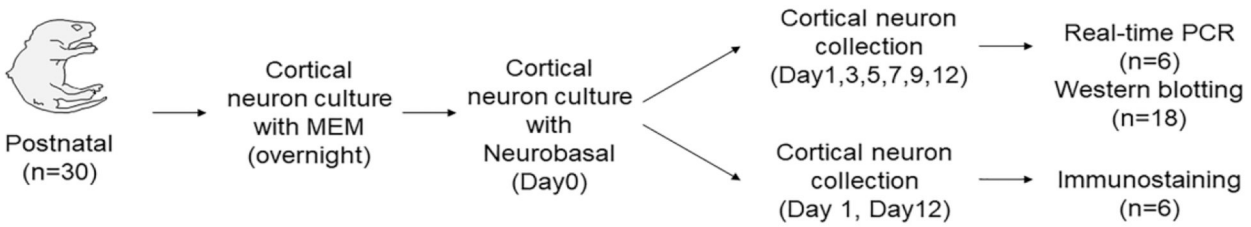

Figure 1. Experimental outline.

A total of 30 postnatal mice were used for preparation of cortical neuron culture. Cortical neurons prepared from 6 mice were used for real-time PCR at Day 1,3,5,7,9,12 after incubation with Neurobasal medium. Cortical neurons prepared from 18 mice were used for western blotting at Day 1,3,5,7,9,12 after incubation with Neurobasal medium. Cortical neurons prepared from 6 mice were used for immunostaining at Day 1 and Day 12 after incubation with Neurobasal medium.

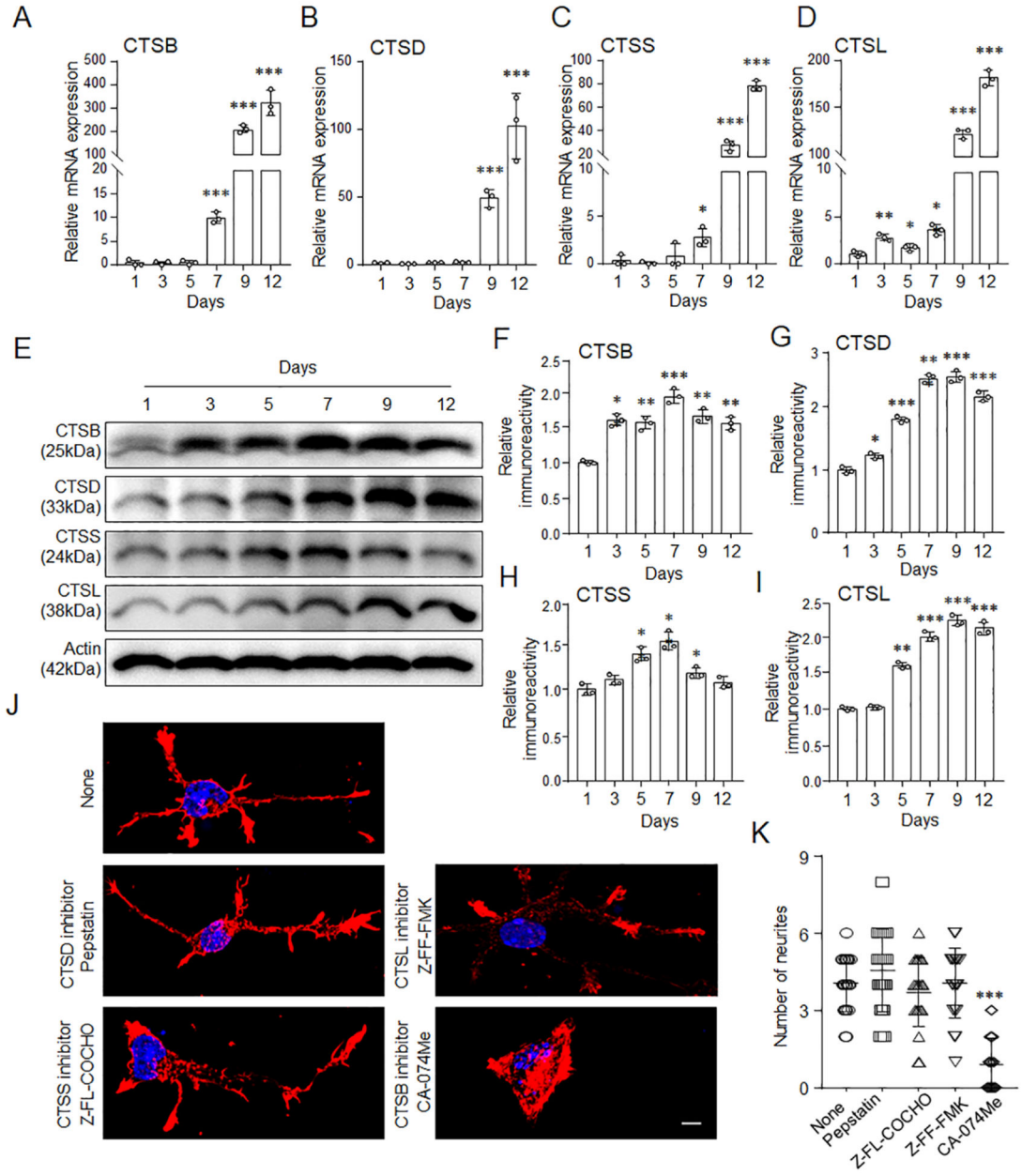

Figure 2. Expression of cathepsins including CTSB were increased during the maturation of primary cortical neurons.

A-D, The mRNA expression of CTSB (A), CTSD (B), CTSS (C) and CTSL(D) in the primary cortical neurons at days in vitro (DIV) 1, 3, 5, 7, 9, 12. The columns and bars represent the means ± SEM (n=3 independent cell culture preparation). The asterisks indicate a statistically significant difference between the values (**P*<0.05, ****P*<0.001, one-way ANOVA test). ***E***, Immunoblottings show CTSB, CTSD, CTSS and CTSL in the primary cortical neurons at days in vitro (DIV) 1, 3, 5, 7, 9, 12. ***F-I***, The quantitative analyses of CTSB (F), CTSD (G), CTSS (H) and CTSL (I) in the immunoblottings of (E). The columns and bars represent the means ± SEM (n=3 independent cell culture preparation). The asterisks indicate a statistically significant difference to the Day 1 group (**P*<0.05,

** $P<0.01$, *** $P<0.001$, one-way ANOVA test). ***J***, Fluorescent images of Filamentous actin (F-actin (red)) and nuclear (blue) in primary neurons at DIV12. The primary neuron were treated with 10 μM Z-FL-COCHO (CTSS inhibitor), 10 μM Pepstatin (aspartyl proteases inhibitor), 10 μM Z-FF-FMK (CTSL inhibitor) and 10 μM CA-074Me (CTSB inhibitor) 1 day after seeding. Scale bars were 5 μm. *K*, Quantification of the numbers of neurites in the staining of (J), Values are represent the means ± SEM (n=20 indicated 20 cells from 3 independent cell culture preparation).

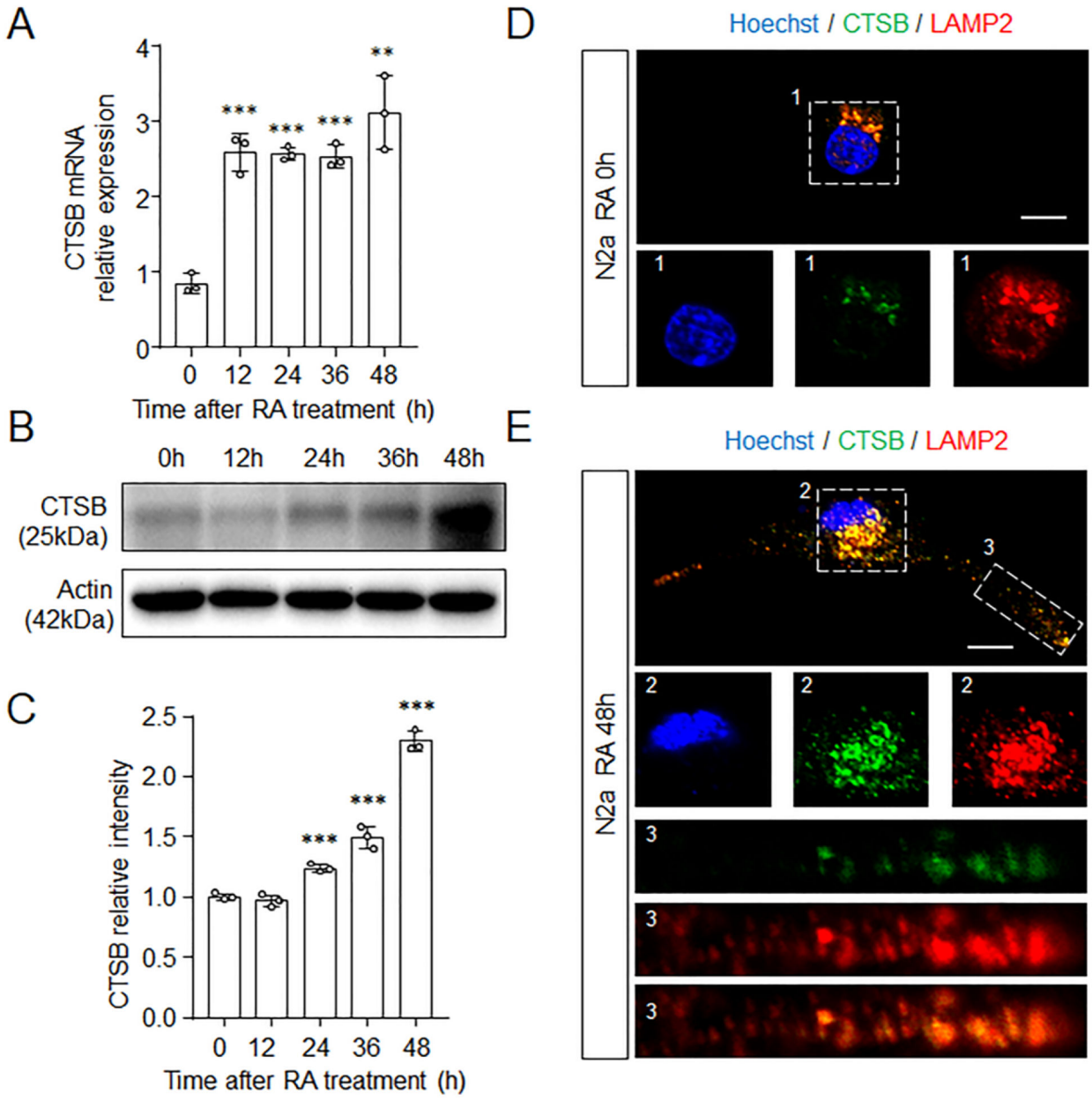

Figure 3. CTSB increased in the somas and neurites of N2a cells after treatment with RA.

A, The mRNA expression of CTSB in N2a cells at 12, 24, 36 and 48h after treatment with RA. ***B***, Immunoblottings show CTSB in N2a cells at 12, 24, 36 and 48h after treatment with RA. ***C***, The quantitative analyses of CTSB in the immunoblottings of (B). The columns and bars represent the means ± SEM (n=3 independent cell culture preparation). The asterisks indicate a statistically significant difference to the 0h group (***P*<0.01, ****P*<0.001, one-way ANOVA test). ***D***, ***E***, Immunofluorescent images of CTSB (Green) and LAMP2 (Red) in N2a cells without RA (D) or 48h with RA treatment (E). Nuclear was stained by Hoechst (Blue). Scale bar, 10μm. Higher magnification of corresponding numbered area (inset1–3) were showed in the bottom panel of each image. Inset 1 and 2 showed the lysosome

localization of CTSB in the cell body of N2a cells without and with RA treatment, Inset 3 showed the lysosome localization of CTSB in the neurite of N2a cells with RA treatment.

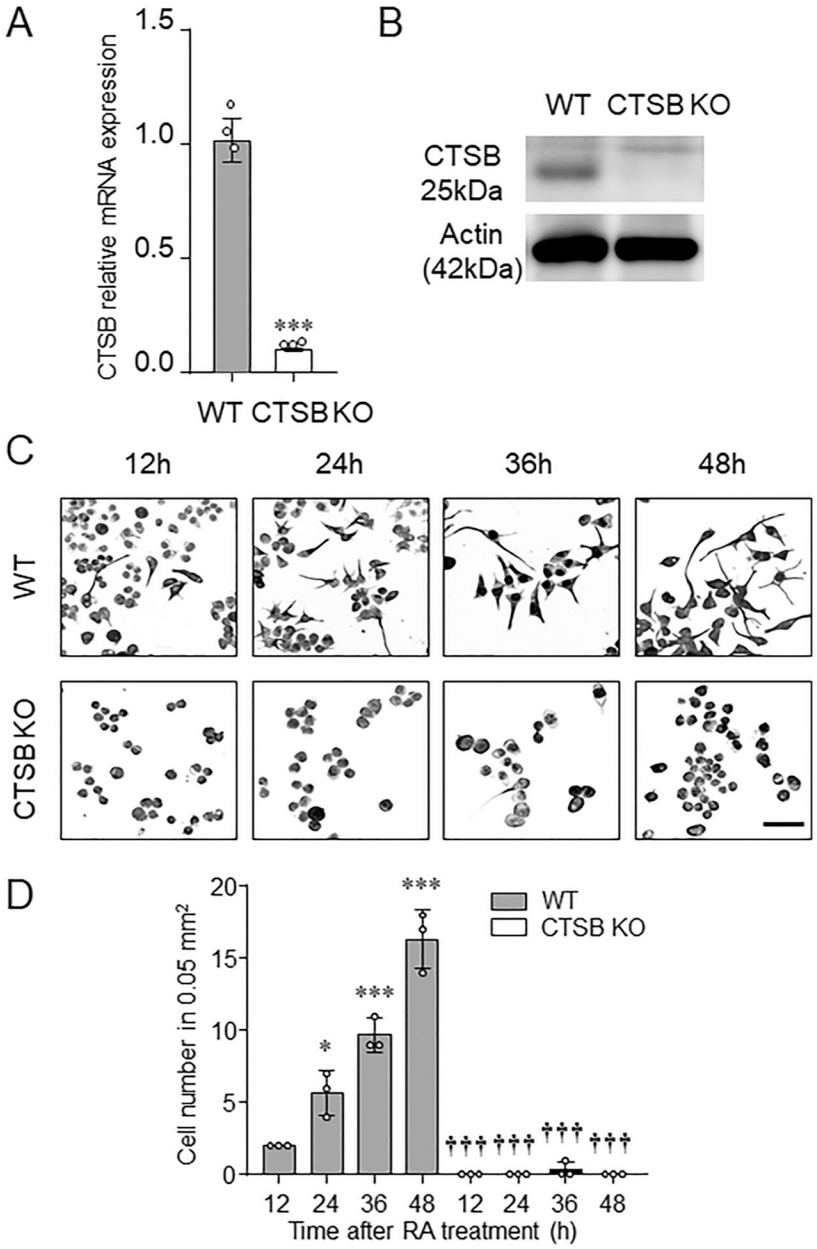

Figure 4. CTSB was involved in neurite outgrowth in N2a cells.

A, The mRNA expression of CTSB in WT and CTSB KO N2a cells. The columns and bars represent the means ± SEM (n=3 independent cell culture preparation). The asterisks indicate a statistically significant difference between the WT group (***P<0.001, student's t test). ***B***, Immunoblottings show CTSB in WT and CTSB KO N2a cells. ***C***, Immunofluorescent images of Neuron-Chrom™ Pan Neuronal Marker in WT and CTSB KO N2a cells at 12, 24, 36 and 48 h after treatment with RA. Scale bar, 50 μm. ***D***, Number of cells exhibiting neurites in the images of (C). The columns and bars represent the means ± SEM (n=6 indicated area of pictures). The asterisks indicate a statistically significant difference from the WT 12h values (*P<0.05, ***P<0.001, one-way ANOVA test). The

daggers indicate a statistically significantly difference between CTSB KO and WT groups at the same time points (†††P<0.001, one-way ANOVA test).

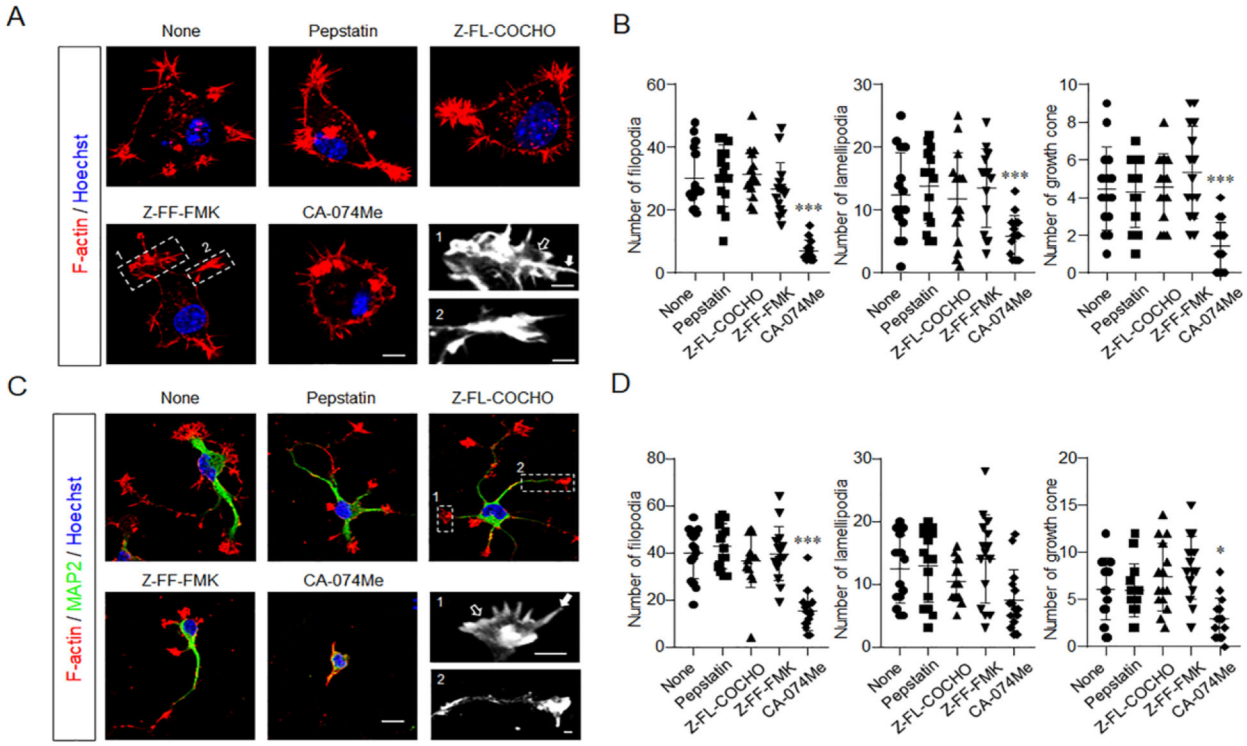

Figure 5. Neurite outgrowth initiation was inhibited by CTSB inhibitor.

(A) Fluorescent images of Filamentous actin (F-actin (red)) and nuclear (blue) in N2a cells at 2 h after treatment with RA. The N2a cells were treated with 10 μM Z-FL-COCHO (CTSS inhibitor), 10 μM Pepstatin (aspartyl proteases inhibitor), 10 μM Z-FF-FMK (CTSL inhibitor) and 10 μM CA-074Me (CTSB inhibitor) 1 h before RA treatment. Scale bars were 5 μm. Bottom right were typical filopodia (Inset 1, white arrow), lamellipodia (Inset 1, open arrow) and growth cone (Inset 2) in N2a cells. Scale bars were 1μm. (B) Quantification of number of filopodia, lamellipodia and growth cone in N2a cells after treatment with inhibitors. Values are represent the means ± SEM (n=15 indicated 15 cells from 3 independent cell culture preparation). The asterisks indicate a statistically significant difference from the None values (***P<0.001, one-way ANOVA test). (C) Fluorescent images of Filamentous actin (F-actin (red)) and nucleus (blue) in primary neurons at DIV1 after incubated with neurobasal medium. The primary neurons were treated with 10 μM Z-FL-COCHO (CTSS inhibitor), 10 μM Pepstatin (aspartyl proteases inhibitor), 10 μM Z-FF-FMK (CTSL inhibitor) and 10 μM CA-074Me (CTSB inhibitor) at DIV0. Scale bars were 10 μm. Bottom right were typical filopodia (Inset 1, white arrow), lamellipodia (Inset 1, open arrow) and growth cone (Inset 2) in primary neurons, Scale bars were 1μm. (D) Quantification of number of filopodia, lamellipodia and growth cone in primary neurons after treatment with inhibitors. Values are represent the means ± SEM (n=15 indicated 15 cells from 3 independent cell culture preparation). The asterisks indicate a statistically significant difference from the None values (*P<0.05, ***P<0.001, one-way ANOVA test).

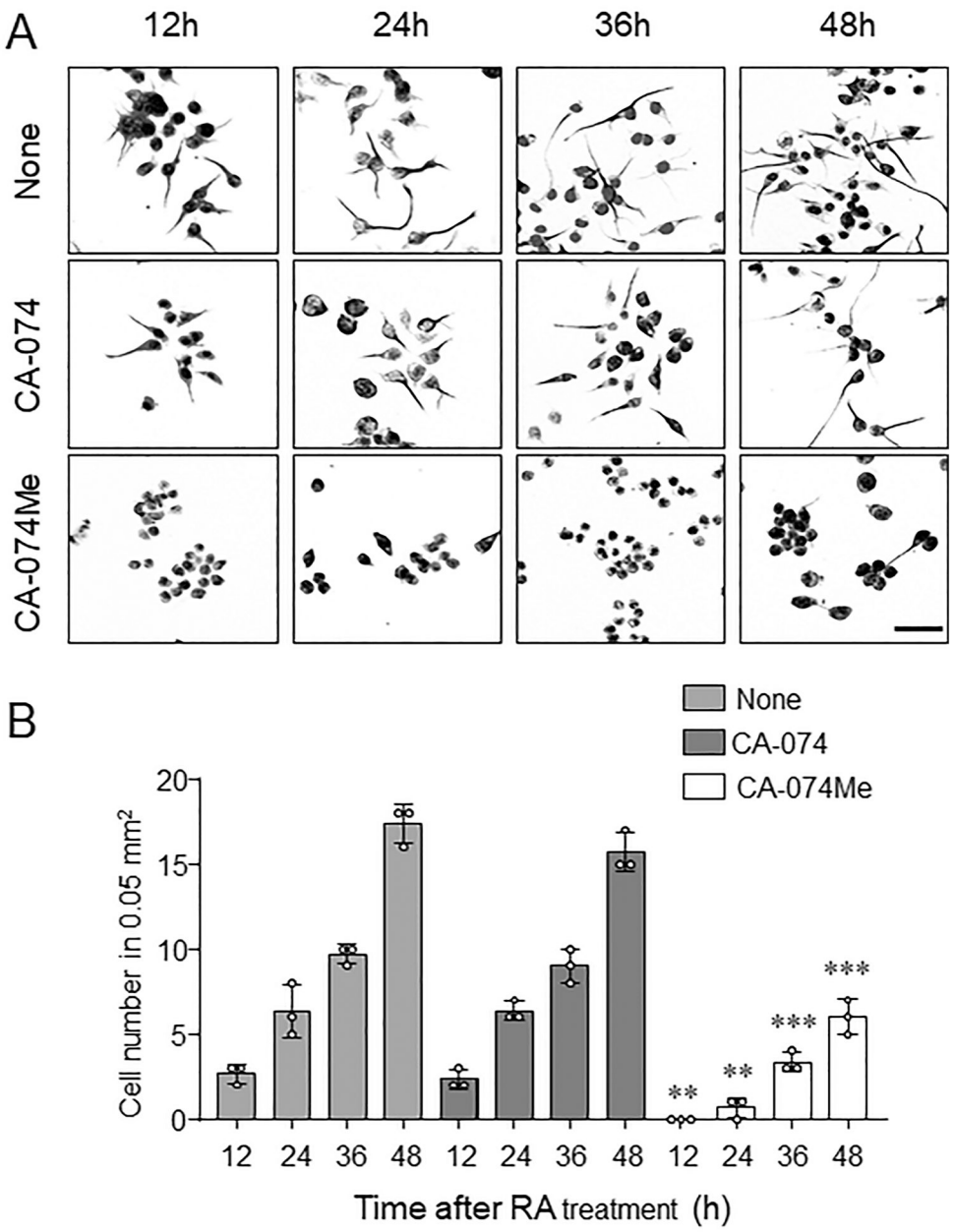

Figure 6. Neurite initiation was regulated by intracellular, but not secretory CTSB.

A, Immunofluorescent images of Neuron-Chrom™ Pan Neuronal Marker in N2a cells at 12, 24, 36 and 48 h after treatment with RA with or without pre-treatment with 10 μM CA074 (none cell-permeable) or 10 μM CA074-Me (cell-permeable). Scale bar, 50 μm. ***B***, Number of cells exhibiting neurites in the images of (A). The columns and bars represent the means ± SEM (n=6 indicated area of pictures). The asterisks indicate a statistically significant difference between the CA-074Me and None groups at the same time points (** $P<0.01$, *** $P<0.001$, one-way ANOVA test).

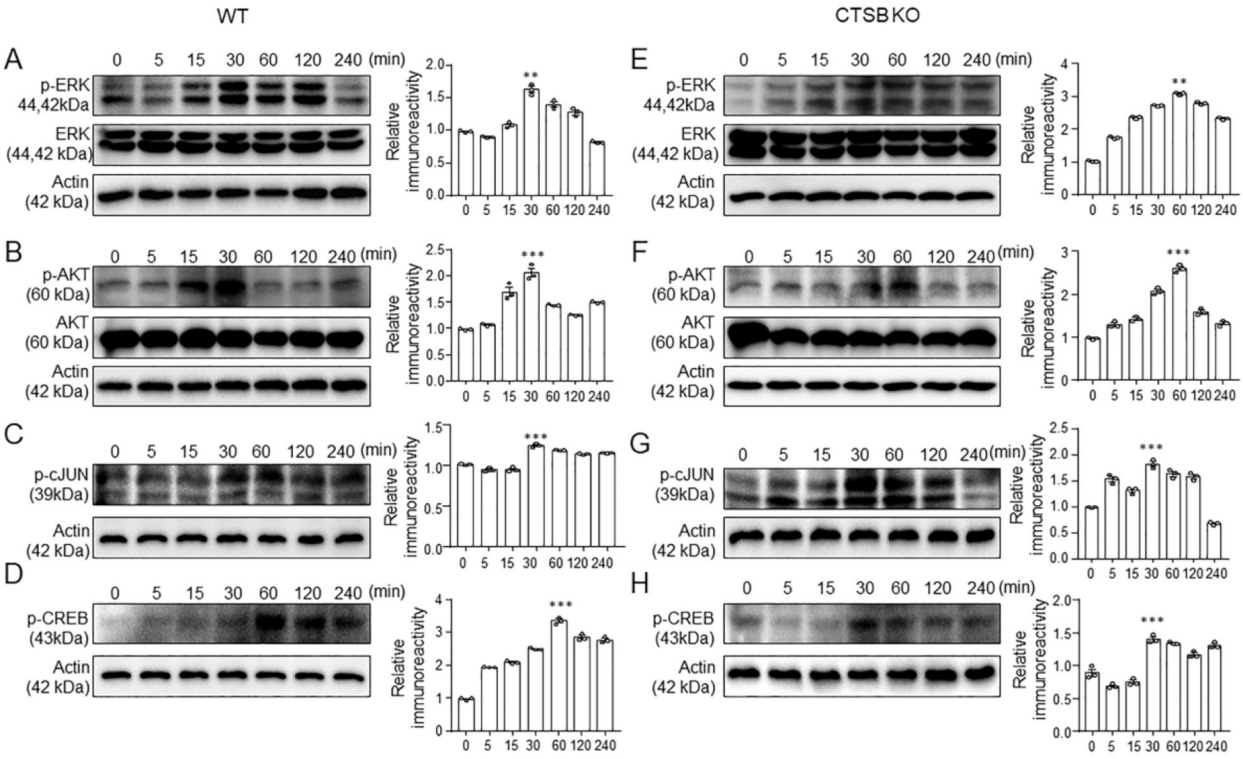

Figure 7. Activation of the signaling pathway by RA treatment in WT and CTSB KO N2a cells.

A-D, Immunoblottings of p-ERK (A), p-AKT (B), p-cJUN (C) and p-CREB (D) in WT N2a cells at 0, 5, 15, 30, 60, 120 and 240min after treatment with RA. The right panel were the quantitative analyses of the left blottings. ***E-H***, Immunoblottings of p-ERK (E), p-AKT (F), p-cJUN (G) and p-CREB (H) in CTSB KO N2a cells at 0, 5, 15, 30, 60, 120 and 240 min after treatment with RA. The right panel were the quantitative analyses of the left blottings. The columns and bars represent the means ± SEM (n=3 independent cell culture preparation). The asterisks indicate a statistically significant difference to the 0h group (** P<0.01, *** P<0.001, one-way ANOVA test).

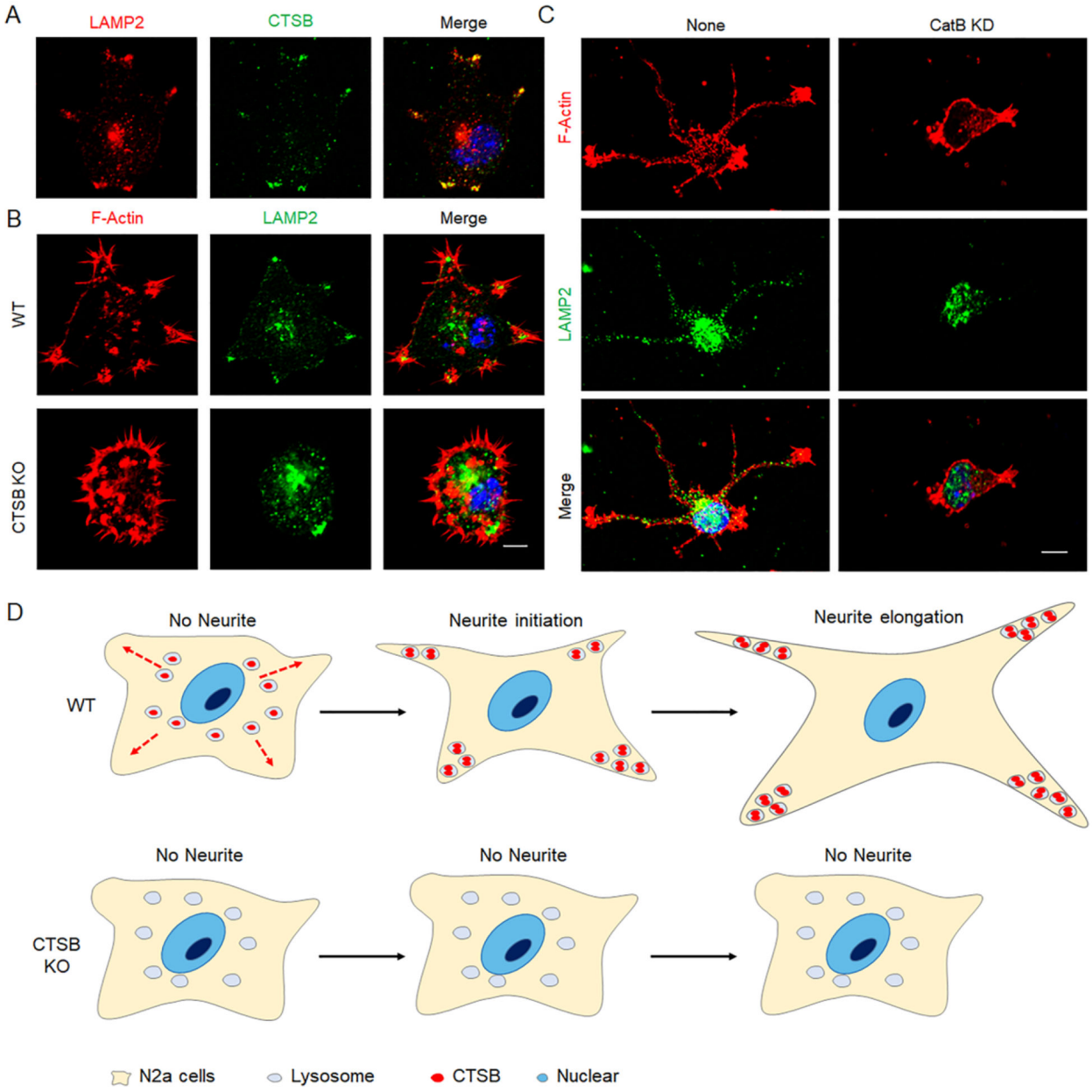

Figure 8. CTSB deficiency failed to traffic lysosomes to the leading edge of neurites.

A, Immunofluorescent images of LAMP2 (red) and CTSB (green) in WT N2a cells at 2 h after treatment with RA. Scale bar, 5 μm. ***B***, Fluorescent images of F-actin (red) and LAMP2 (green) in WT and CTSB KO N2a cells at 2 h after treatment with RA. Scale bar, 5 μm. ***C***, Fluorescent images of F-actin (red) and LAMP2 (green) in WT and CTSB KD primary neurons at DIV1 after incubated with neurobasal medium. Scale bar, 10 μm. ***D***, Schematic illustration of neurite outgrowth in N2a cells. WT N2a cells show increased expression of CTSB during development which lead the lysosomes trafficking and remodeling at the cell edge, followed by neurite initiation and elongation. CTSB KO N2a cells show cytosol distribution of lysosomes with no neurites during development.